Regulation of CTP: Phosphocholine Cytidylyltransferase Activity by the Physical Properties of Lipid Membranes: An Important Role for Stored Curvature Strain Energy†

Sarah M. A. Davies,‡,§ Richard M. Epand,|| Ruud Kraayenhof,⊥ and Rosemary B. Cornell*,‡

Department of Molecular Biology and Biochemistry, Simon Fraser University, Burnaby, British Columbia, V5A 1S6, Canada, and Department of Biochemistry, McMaster University Health Sciences Centre, 1200 Main Street West, Hamilton, Ontario, L8N 3Z5, Canada, and Institute of Molecular Biological Sciences, BioCentrum Amsterdam, Vrije Universiteit, De Boelelaan 1087, 1081 HV Amsterdam, The Netherlands

Received May 2, 2001; Revised Manuscript Received July 10, 2001

ABSTRACT: CTP:Phosphocholine cytidylyltransferase (CT) catalyzes the key step in phosphatidylcholine (PC) synthesis. CT is activated by binding to certain lipid membranes. The membrane binding affinity of CT can vary from micromolar to millimolar K_d, depending on the lipid composition of the target membrane. Class II CT activators like diacylglycerols and unsaturated phosphatidylethanolamines (PE) favor inverted lipid phase formation. The mechanism(s) governing CT's association with class II lipid membranes and subsequent activation are relatively unknown. We measured CT activation by vesicles composed of PC and one of three unsaturated PEs, dioleoylglycerol (DOG), or cholesterol. For each lipid system, we estimated the stored curvature strain energy of the monolayer when confined to a relatively flat bilayer. CT binding and activation correlate very well with the curvature strain energy of several chemically distinct class II lipid systems, with the exception of those containing cholesterol, in which CT activation was less than the increase in curvature strain. CT activation by membranes containing DOG was reversed by inclusion of specific lysolipids, which reduce curvature strain energy. LysoPC, which has a larger positive curvature than lysoPE, produced greater inhibition of CT activation. Stored curvature strain energy is thus an important determinant of CT activation. Membrane interfacial polarity was investigated using a membrane-anchored fluorescent probe. Decreases in quenching of this interfacial probe by doxyl-PCs in class II membranes suggest the probe adopts a more superficial membrane location. This may reflect an increased surface hydrophobicity of class II lipid membranes, implying a role for surface dehydration in CT's interactions with membranes containing class II lipids. Cholesterol, a poor activator of CT, did not affect the positioning of the polarity-sensitive probe, suggesting that one reason for its ineffectiveness is an inability to enhance surface hydrophobicity.

Cell membranes have distinct and highly regulated lipid compositions. In eukaryotes, the phosphatidylcholine (PC)[1] content of cell membranes is kept fairly constant, despite changes in the PC turnover rate (*1*). Clearly, lipid homeostasis in cells is crucial to cell survival and to the maintenance of optimally functioning biological membranes. There is now much evidence suggesting that several membrane physical properties are tightly regulated in bacteria, including the negative charge density and stored curvature strain energy (*2-4*). This can be achieved by the sensitivity of key enzymes in lipid synthesis to perturbations in lipid packing (*5*, *6*). In eukaryotes, increasing evidence supports a regulatory role for membrane physical properties in the functioning of membrane proteins (*7*−*12*).

CT catalyzes the main regulatory and rate-limiting step in the de novo synthesis of PC in higher animal and plant cells (*13*). PC is the most abundant lipid in mammalian cell membranes, where it plays an important role in stabilizing the bilayer phase of biological membranes. CT is present in cells in both a soluble form and a membrane-bound form. The soluble form has extremely low activity; membrane binding is accompanied by activation, whereby K_{cat} increases

† This work was supported by The Wellcome Trust and the Canadian Institutes of Health Research. S.M.A.D. is an International Wellcome Fellow.

* To whom correspondence should be addressed. E-mail: cornell@sfu.ca. Phone: (604) 291-3709. Fax: (604) 291-5583.

‡ Simon Fraser University.

§ Present address: Department of Preclinical Veterinary Sciences, R.(D).S.V.S., Summerhall, University of Edinburgh, Edinburgh, EH9 1QH, U.K.

|| McMaster University Health Sciences Centre.

⊥ Vrije Universiteit.

[1] Abbreviations: CT, CTP:phosphocholine cytidylyltransferase; CTP, cytidine triphosphate; DAG, diacylglycerol; DOG, dioleoylglycerol; DOPC, dioleoyl-PC; DOPE, dioleoyl-PE (Δ9); 5-doxyl-PC, 1-palmitoyl-2-stearoyl-(5-doxyl)PC; 7-doxyl-PC, 1-palmitoyl-2-stearoyl-(7-doxyl)PC; 10-doxyl-PC, 1-palmitoyl-2-stearoyl-(10-doxyl)PC; DPLPE, dipetroselinoyl-PE (Δ6); DPPC, dipalmitoyl-PC; DTMAC, 4-[(*n*-dodecylthio)methyl]-7-(*N*,*N*-dimethylamino)-coumarin; DVPE, divaccenoyl-PE (Δ11); OPC, 1-oleoyl-2-hydroxy-PC; OPE, 1-oleoyl-2-hydroxy-PE; PC, phosphatidylcholine; PE, phosphatidylethanolamine; POPE, 1-palmitoyl-2-oleoyl-PE; PS, phosphatidylserine; DTT, dithiothreitol; EDTA, ethylenediaminetetraacetic acid; LUVs, large unilamellar vesicles; K_c, elastic bending modulus; R_o, intrinsic radius of curvature; T_H, bilayer-to-hexagonal phase transition temperature; PKC, protein kinase C; TLC, thin-layer chromatography.

10.1021/bi010904c CCC: $20.00
Published on Web 08/08/2001

by up to 80-fold (*14*), and K_m for the substrate CTP is reduced by 20−30-fold (*15*). The interconversion between these two cellular pools is central to the regulation of CT activity (*16*).

The association of CT with cell membranes is weak and reversible. To date, no membrane protein receptors have been identified for CT. Rather, CT likely interacts directly with the lipids of cell membranes. The lipid composition of a membrane is a major determinant of CT-membrane association (*13*). Evidence suggests that CT senses physical properties of the membrane that accompany PC deficiency (*16*−*18*). CT does not have a specific binding site for a lipid monomer. Instead, its membrane-binding domain (domain M), a single, long, uninterrupted amphipathic α-helix (*19*), partitions into the membrane phase, contacting multiple lipids (*17*, *20*). The extent of this partitioning is determined by the intrinsic solubility of domain M for the lipid vs aqueous phase.

Studies both in vivo and in vitro have identified two chemically diverse classes of lipid activators whose presence in membranes promote CT's binding and subsequent activation (e.g., *21*−*29*). Class I activators include anionic lipids and fatty acids, while class II includes diacylglycerols (DAG) and unsaturated phosphatidylethanolamines (PE). Electrostatic interactions between the negatively charged headgroups of class I lipid molecules and the positively charged amino acids in domain M of CT are thought to promote CT's membrane binding (*27*). Little is known about CT activation by membranes containing class II lipids (also known as *type II* lipids), which tend to promote nonlamellar phases. The idea of regulation of CT's membrane affinity by the ratio of nonlamellar forming to lamellar lipids was first explicitly stated by Jamil et al. (*30*) in 1993, and expanded by Cornell and Arnold in 1996 (*18*). Using choline-starved cells treated with phospholipases, Jamil et al. correlated increased partitioning of CT to cellular membranes with decreased membrane PC content relative to the other lipid classes (*30*). Choline supplementation of the cells increased membrane PC and reduced the CT-membrane partitioning. They also discovered that lysoPC could reverse the effects of phospholipase C on the membrane affinity of CT (*30*). An interpretation of this observation is that the lysoPC, a type I lipid, could antagonize the effects of the type II lipid, DAG, produced by the phospholipase C treatment. Recently Attard et al. (*31*) proposed that CT responds to the negative curvature strain of membranes containing type II lipids. They modeled the activation of purified CT by DOPE as a component of DOPC vesicles to the calculated stored curvature strain as a function of increasing DOPE. They also showed antagonism between DOPE and several type I lipids toward CT activity (*31*).

The aim of our study was to further explore this relationship and to determine which specific physical properties of class II lipid membranes are responsible for regulating CT activity. Figure 1 illustrates some physical properties of membranes containing class II lipids that may affect CT activity. As the content of a class II lipid increases in a membrane, it gains a tendency for each of the monolayers to curl toward the water (negative curvature, Figure 1A). The curling tendency can be rationalized with a simple descriptive model that considers the overall shape of class II lipid molecules (*32*). The cross-sectional area of the

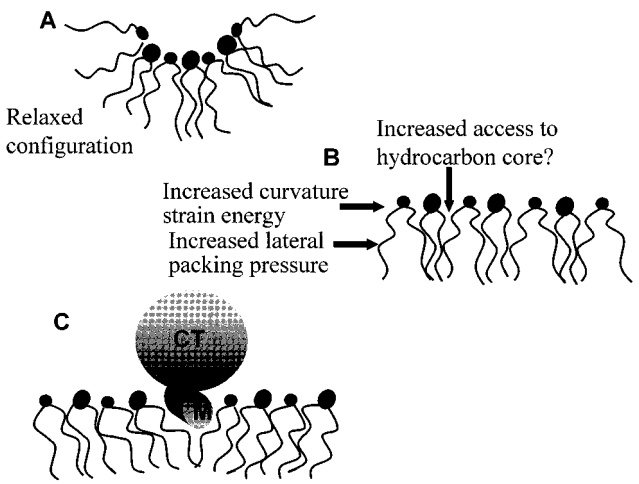

FIGURE 1: Schematic diagram illustrating physical properties of class II lipid membranes that might regulate membrane binding and subsequent activation of CT. (A) The lowest curvature energy of a class II lipid is as a monolayer with negative curvature. (B) Forcing class II lipids into a relatively flat configuration, such as a biological membrane or LUV, increases the potential energy within the bilayer, the stored curvature strain energy. There may also be more voids, lipid "packing defects", present in the membrane interfacial region, and increased lateral packing pressure. (C) Which particular membrane physical properties account for CT's activation by class II lipid membranes? Relief of stored curvature strain energy when domain M of CT inserts into the superficial region of the lipid bilayer? Facilitation of domain M's intercalation into the membrane interface by "packing defects"?

headgroup region is small relative to the cross-sectional area of the acyl chain region. This gives rise to negative lateral pressure at the surface and positive lateral pressure in the acyl chain region (*33*). The curling drive is a response to minimize packing voids at the surface while maximizing the free volume of the acyl chains. If the monolayers are prevented from curling by being constrained in a bilayer, latent free energy will be stored within the membrane (Figure 1B). This stored curvature strain energy can be quantified according to a quadratic function. We have adopted the relationship derived by Helfrich (*34*) and used by Gruner et al. (*35*), Rand et al. (*36*), and Nielsen and Andersen (*37*), which defines the stored curvature strain energy as

$$\frac{0.5K_c}{R_0^2} \qquad (1)$$

per unit area of interface, where K_c is the elastic bending modulus of the lipid monolayer and R_0 is the lipid monolayer's spontaneous radius of curvature in excess water. This definition holds true only if there is no local physical curvature of the membrane and no compositional asymmetry across the two monolayers of the bilayer.

When CT binds to a lipid membrane, domain M of CT is believed to lie relatively parallel to the membrane surface, its hydrophobic face buried in the hydrophobic region of the lipid membrane (*20*, *38*), and its hydrophilic face still in contact with the aqueous phase. Using brominated lipids as depth quenchers of peptide tryptophan residues, domain M peptide has been shown to intercalate no more than halfway into the outer monolayer of lipid vesicles (*38*). Insertion of domain M of CT into the more superficial regions of a class II lipid monolayer might relieve the stored curvature strain

energy of that monolayer, allowing the system to move to a lower free energy state (Figure 1C). Furthermore, interaction with a class II membrane might liberate free energy that could be used to induce a conformational change in CT.

Another potential consequence of forcing class II lipids into a flat bilayer may be the production of "packing defects" within the membrane (Figure 1B). The relatively small headgroups of class II lipids render them effective "spacer" molecules: increasing the separation between neighboring phospholipid headgroups and reducing intermolecular interactions (*39*). CT must intercalate into a lipid membrane in order to become activated (*26*, *27*). Furthermore, the hydrophobic driving force has been shown to dominate CT-membrane interactions (*27*). Thus, more loosely packed membranes that facilitate the penetration of the enzyme's hydrophobic side chains into the membrane's hydrophobic interior should increase CT activation. In support of this, CT is not greatly activated by highly ordered, tightly packed bilayers, but pure PC membranes can be transformed from relatively inert to active binding surfaces for CT by oxidation of double bonds in the PC acyl chains, which is thought to decrease lipid packing density (*40*).

In this study, we used a model membrane system of 100 nm diameter large unilamellar vesicles (LUVs), as vesicles of this size have no local geometric curvature but still have a relatively uniform size distribution (*41*). Component lipids were chosen for which values of K_c and R_o were available. The CT used in our study was purified by a method that produces lipid-free and detergent-free enzyme *(14*), which is ideal for studies of regulation by exogenous lipids. The stored curvature strain energies of the different lipid systems were estimated and then correlated with the amount of CT activation. The polarity of the membrane interface and the access for CT to the bilayer interior were estimated by measuring the quenching of the fluorescent probe 4-[(*n*-dodecylthio)methyl]-7-(*N*,*N*-dimethylamino)coumarin (DTMAC) by doxyl groups positioned at various depths within the membrane, and these were also compared to CT activation.

EXPERIMENTAL PROCEDURES

Materials. We used only di-18:1 phospholipids to minimize chain mismatch effects. All lipids (Avanti Polar Lipids, Alabaster, AL) were >99% pure as determined by thin-layer chromatography (TLC) using chloroform/methanol/ammonia (65:35:5). Less than 1% of dioleoylglycerol (DOG) was the 1,3 isoform, as determined by TLC, using hexane/diethyl ether/acetic acid (60:40:1). Lipids were stored as stock solutions in chloroform under argon at −20 °C. The concentrations were determined regularly by phosphate assay (*42*). [methyl-^{3}H]Choline chloride, [^{3}H]dipalmitoylphosphatidylcholine ([^{3}H]DPPC), and [^{14}C]phosphocholine were from New England Nuclear (Boston, MA) and Amersham Pharmacia Biotech (Quebec). [^{3}H]Phosphocholine (specific radioactivity = 10−15 Ci/mol) was prepared from [^{3}H]choline as described previously (*43*). Cytidine triphosphate (CTP), dithiothreitol (DTT), CM-Sepharose, DEAE-Sepharose, Tris, NaCl, and Nonidet P-40 were from Sigma-Aldrich Canada Co. All other chemicals were of reagent-grade. Microcon 100 centrifugal filter devices were from Millipore (Amicon Bioseparations). The synthesis of 4-[(*n*-dodecylthio)methyl]-7-(*N*,*N*-dimethylamino)coumarin (DTMAC) has been described previously (*44*).

Methods. Purification of CT. Rat liver CTα was expressed in *Trichoplusia* ni cells. These cells were lysed and the cytosol was prepared as described previously (*45*). CT was then purified according to the method of Friesen et al. (*14*), with the following modifications. The DEAE column (20 mL resin/40 mL cytosol) was washed with 5 column volumes each of buffer A (10 mM Tris, pH 7.5, 1 mM EDTA, and 2 mM DTT) containing 150 mM NaCl and 1% NP-40, and buffer B containing 150 mM NaCl prior to elution of CT as described. The CM-Sepharose column (10 mL resin/40 mL cytosol) was washed with 2−3 column volumes of buffer A containing 30 mM NaCl and then eluted with 4 column volumes of buffer A containing 150 mM NaCl. Pure enzyme was stored in small aliquots at −80 °C. For each experiment, a fresh aliquot was thawed rapidly at 37 °C and kept on ice during sample preparation.

Preparation of 100 nm Large Unilamellar Vesicles (LUVs). Lipid mixtures were dried under nitrogen gas and placed under vacuum overnight to remove trace residual solvent. The resulting lipid films were suspended in liposome buffer (20 mM Tris and 1 mM EDTA, pH 7.4) and vortexed vigorously at room temperature. They were then subjected to five freeze−thaw cycles using liquid nitrogen, followed by 19 extrusions through two stacked 0.1 μm pore polycarbonate filters in a Liposofast microextruder (Avestin Inc., Ottawa, ON). The size distributions of the resultant LUV populations were measured using a Nicomp model 270 particle sizer (Nicomp Instruments Inc., Goleta, CA). In all experiments, the measured mean diameter and size distribution of the LUV populations were not significantly affected by lipid composition. Vesicles were always used within 6 h of preparation.

CT Activity Assays. CT's conversion of phosphocholine to CDP-choline was measured in the presence of LUVs of specific lipid compositions. The reaction mixture contained 30 mM Tris, pH 7.4, 12 mM $MgCl_2$, 10 mM CTP, 10 mM DTT, 250 μM EDTA, 88 mM NaCl, and 0.11 μg of CT, and 1.6 mM labeled phosphocholine, in a final volume of 50 μL. [^{14}C]Phosphocholine (specific radioactivity = 2 Ci/mol) or [^{3}H]phosphocholine (specific radioactivity = 10 Ci/mol) was added to start the reaction. After 15 min in a shaking water bath, the reaction was stopped by adding 30 μL of methanol/ammonia (9:1) solution. The amount of [^{3}H]CDP-choline or [^{14}C]CDP-choline formed was determined by TLC separation of substrate and product as described previously (*46*). The specific activity of CT, which is nanomoles of product formed per minute per milligram of CT, was calculated from the measured radioactivity of CDP-choline.

CT Binding Assays. Microcon 100 centrifugal filtration devices were pre-rinsed with buffer (20 mM Tris and 1 mM EDTA, pH 7.4). NaCl was added from a 315.5 mM stock to simulate the ionic strength used in the CT activity assays. The temperatures, durations, DTT concentrations, and lipid:protein molar ratios were also identical to those used in activity assays. Two micrograms of CT was added to the sample, in a final volume of 208 μL. Samples were incubated at the assay temperature for 15 min and then centrifuged at 4 °C and 6100 rpm to give a retentate volume of 13−15 μL. Fractions of the retentate, filtrate, and the excised filter were boiled in SDS-sample buffer (*47*). Quantification of CT in these fractions was obtained,

following electrophoresis on 12% polyacrylamide gels (*47*), by densitometry of the Coomassie-stained gels (Arcus II Agfa Scanner; ScionImage program, NIH). Recovery of CT in all three fractions was ~87−90% of the starting amount. The inclusion of trace amounts of [^{3}H]DPPC in the LUVs and the measurement of ^{3}H dpm in the retentate and filtrate fractions and also on the filter showed that <1% of the lipid was present in the filtrate fraction, and <10% stuck to the filter.

Fluorescence Measurements. LUVs were prepared containing 0.5 mol % DTMAC ± 5 mol % 1-palmitoyl-2-stearoyl-(*n*-doxyl) PC, where $n = 5$, 7, or 10. Fluorescence measurements were made using an SLM 4800C spectrofluorometer (SLM Aminco, Rochester, NY), with a thermoregulated sample cell holder. The excitation wavelength used for DTMAC in LUVs was 397 nm, and the observed emission maxima were 475 ± 6 nm. The excitation and emission slit widths were 4 nm. All values were corrected for background noise from pure lipid LUVs. To check for possible direct chemical interactions between the DTMAC and the doxyl quenchers, and for variation in DTMAC bleaching in the presence of doxyl lipids, a small aliquot of each sample was removed both before and after fluorescence measurements. These aliquots were diluted 9-fold in absolute ethanol, to disrupt the vesicles and so relieve any DTMAC quenching by the doxyl lipids (*48*), and the fluorescence of samples containing DTMAC alone were compared to that of DTMAC in the presence of the doxyl quenchers. The differences were found to be less than 5%, unless stated otherwise.

RESULTS AND DISCUSSION

Activation of CT by Unsaturated PE Correlates with Negative Curvature Strain. Phospholipids containing PE headgroups are the most common class II lipids in animal cell membranes. Some controversy exists regarding PE's ability to activate CT. In one study, liposomes containing DOPE activated rat liver cytoplasmic CT, but had little effect on highly purified enzyme (*29*). Other studies have reported disparately either CT activation (*31*, *49*) or little or no CT activation (*50*) by PE. To clarify this situation, we measured the activation of our highly purified CT by DOPC LUVs containing increasing amounts of DOPE. We used a maximum of 70 mol % PE, as above this PE content the liposomes may become unstable over several hours at room temperature (*51*). Figure 2A shows that unsaturated PE does activate CT and this activation has a sigmoidal dependence on the mol % DOPE. The Hill fit of the data gives a value of 24 mol % for half-maximal activation.

Using the measured values for R_0 and K_c of DOPC (R_0 = 87.3 Å, K_c = 9 kT at 32 °C) (*52*), and DOPE (R_0 = 29.4 Å, K_c = 13 kT at 22 °C) (*53*), we estimated the stored curvature strain energy for LUVs of varying mol %s DOPE. The CT activity assay temperature, 25 °C, and the temperatures at which the values for R_0 of DOPC and DOPE were measured, 32 and 22 °C respectively, are not identical. However, we expect this effect on the overall accuracy of our calculation to be small: R_0 of DOPE has been shown to change by only 1−1.5 Å (~4%) with a 10 °C change in temperature (*53*). Moreover, the effect of R_0 on the lamellar-to-inverse hexagonal phase transition temperature (T_H) has been demonstrated successfully, without correcting for the temperature dependence of R_0 (*54*). R_0 is considered to be a colligative property of a mixed lipid monolayer (*55*, *56*), and this has been demonstrated both theoretically and experimentally (*36*, *54*, *56*) for mixtures of DOPC and DOPE. For DOPC-DOPE systems, the curvature stress values of the individual components are also approximately additive (*54*). We therefore estimated the stored curvature strain energy of our lipid systems according to the mole fractions of each lipid component present, using eq 1.

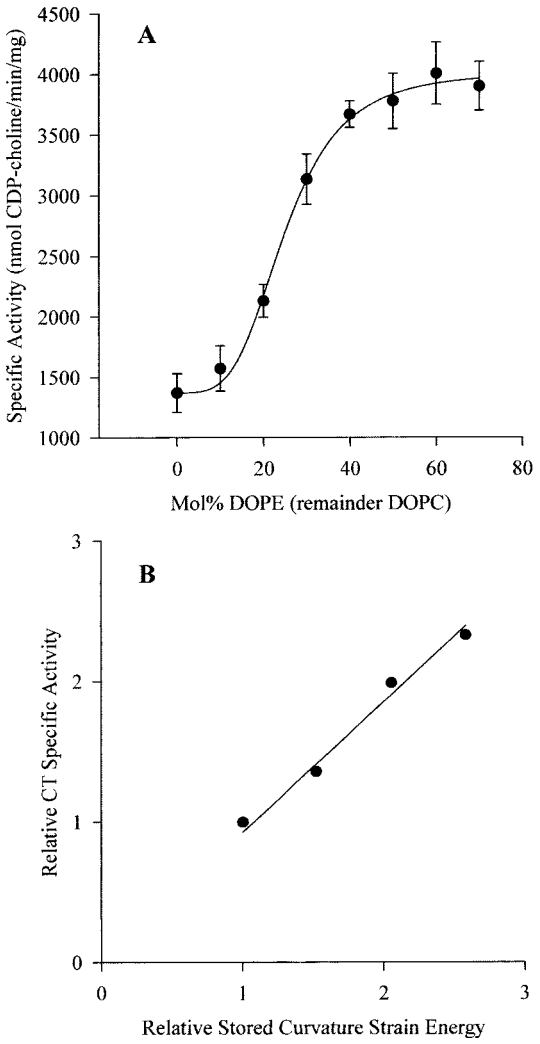

FIGURE 2: (A) Activation of CT by DOPE. CT activity was measured in the presence of DOPC LUVs containing 0−70 mol % DOPE (400 μM total lipid) at 25 °C. Error bars represent the standard error of the mean of two experiments performed in triplicate. Curve shown is the Hill-Langmuir fit of the data. (B) Correlation between the calculated stored curvature strain energy of DOPC/DOPE LUVs and their activation of CT at 25 °C. The relative stored curvature strain energy values shown are for 10−40 mol % DOPE LUVs (the linear region of Figure 2A) and are normalized to that of 10% DOPE, which is assigned the value of 1.00 (see text for details on calculations). The relative activity values are calculated from the data shown in Figure 2A, scaled to a value of 1.00 for CT activation by 10 mol % DOPE LUVs. $r^2 = 0.99$, $P < 0.05$.

Figure 2B shows the correlation between the calculated relative stored curvature strain energy of DOPC/DOPE LUVs and the relative activation of CT, for mole percents of DOPE that fall within the linear section of the activation curve. The

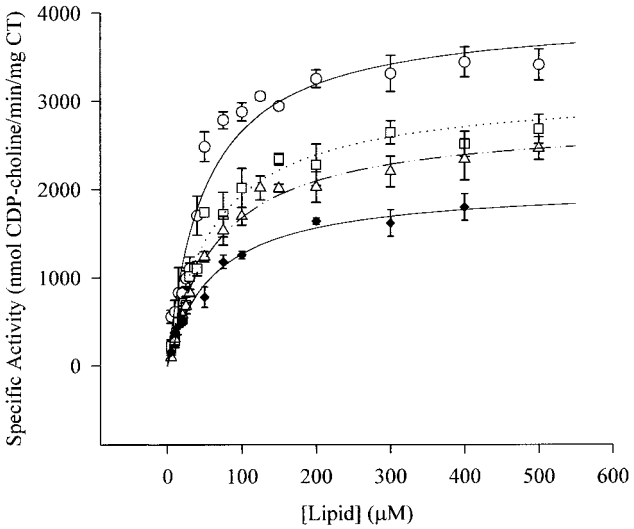

FIGURE 3: Activation of CT by DOPC LUVs containing 60% of a particular di-18:1 PE: Δ6 (□), Δ9 (○), and Δ11 (△) at 25 °C. Curves represent data fits to the Hill-Langmuir equation. Error bars represent the standard error of the mean of three independent experiments done in triplicate. CT activation by pure DOPC LUVs (◆) at 25 °C is also plotted for comparison. DOPC data error bars represent the standard error of the mean of two separate experiments done in triplicate.

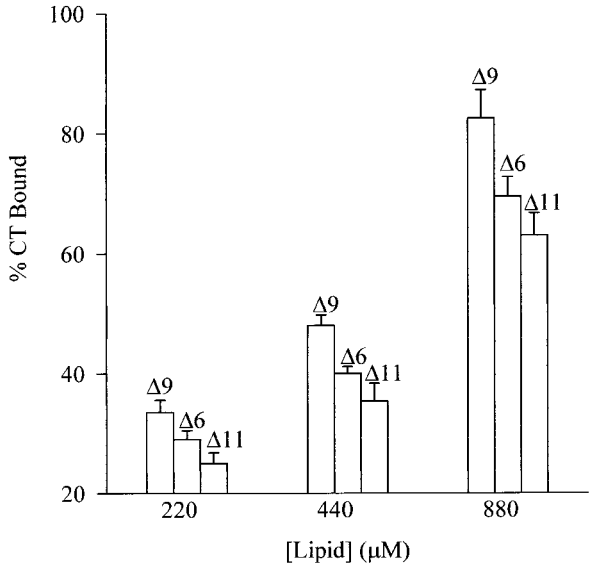

FIGURE 4: CT binding at 25 °C to 220, 440, and 880 μM DOPC LUVs containing 60% of each di-18:1 PE. The particular PE is indicated above the data. Error bars represent the standard error of the mean of three independent experiments.

association between these two variables appears to show a very high degree of correlation in this region. These results suggest a major role for stored curvature strain energy in the activation of CT by DOPC/DOPE lipid bilayers.

In the above study, CT activation could depend entirely on specific interactions between CT and phosphoethanolamine. To distinguish between the requirement for a specific chemical group and the effects of membrane physical properties, we measured the relative membrane-binding and activation of CT using vesicles composed of DOPC with a series of three di-18:1 PE lipids. Dipetroselinoyl-PE (DPLPE, Δ6), dioleoyl-PE (DOPE, Δ9), and divaccenoyl-PE (DVPE, Δ11), are chemically identical, apart from the position of the double bond in their acyl chains. The values for R_0 and K_c of these three PEs have been measured previously and were found to differ (*57*). Figure 3 shows the activation of CT by LUVs composed of 60 mol % of each PE and 40 mol % DOPC, as a function of total lipid concentration, at 25 °C. We chose 60 mol % PE as our lipid composition, since this gave virtually maximal CT activation for the DOPC/DOPE lipid system (Figure 2A), while also ensuring the presence of a stable bilayer configuration at room temperature (*51*). The activation of CT by pure DOPC LUVs at 25 °C is also shown for comparison. The maximum CT activation produced by 60% DOPE (Δ9) LUVs was approximately 80% greater than that seen with pure DOPC LUVs. CT activation by 60% DOPG LUVs was also measured at 25 °C for a comparison with a potent class I activator; maximal CT activation was found to be 3.5−4-fold greater than that seen with pure DOPC LUVs (data not shown).

The relative binding of CT to the different PC/di-18:1 PE LUVs was also measured by a filter trap assay (Figure 4). CT's membrane binding and activation showed the same trend: maximal CT binding and activation were seen with DOPE (Δ9) LUVs, while least binding and activation were observed with DVPE (Δ11) LUVs. The Hill-Langmuir equation was thus used to fit the activity data. Table 1 compares the apparent partition coefficients of CT and the maximal CT activities with the calculated stored curvature strain energies for the three PE systems at 25 °C. Once again, the stored curvature strain energy appears to correlate well with CT activation by these class II lipid systems.

Table 1: Comparison of the Effects of a Series of 60 mol % di-18:1 PE LUVs on the Membrane-Binding and Activation of CT with the Relative Stored Curvature Strain Energies, Calculated Using Equation 1[a]

lipid (di-18:1$_c$ PEs)	relative CT activation	relative CT apparent partition coefficient	relative curvature strain energy
Δ9	1.28	1.23	1.26
Δ6	1.00	1.00	1.00
Δ11	0.89	0.93	0.67

[a] CT maximal activities and CT binding coefficients used in the calculations were derived from the Hill-Langmuir fits to the data shown in Figure 3. All data were obtained at 25 °C and are normalized to the values obtained for Δ6 PE.

Activation of CT by Diacylglycerol Correlates with Negative Curvature Strain. DAGs are important physiological activators of CT (*24*, *58*, *59*). Their activation of CT in vitro requires presentation as a component of a membrane. Micelles containing class II lipids do not activate CT (*25*). Since micelles are devoid of negative curvature strain, this could explain their inability to activate CT. The relevant physical parameters have been measured for dioleoylglycerol (DOG). At 25 °C, R_0 = 11.5 Å for DOG, and R_0 of the mixed DOG-DOPE monolayer is colligative (*60*). An increase in DOG content from 5 to15 mol % increases K_c by ∼7% (*60*). CT activity increased with increasing mol % DOG in DOPC, showing a maximum activity at 15 mol % DOG at 37 °C (data not shown). The Hill fit for the data gave a value of 4 mol % DOG for half-maximal CT activation. This is in excellent agreement with a previous study, using egg PC-derived DAG in egg PC vesicles at 37 °C (*27*). Since the R_0 and K_c data for DOG-containing monolayers were obtained at 25 °C, we also performed CT activity experiments at this temperature, and CT activity

Table 2: Comparison of the Effects of 5−15 mol % DOG in DOPC LUVs on the Stored Curvature Strain Energy and on CT Activation[a]

mol % DOG	relative curvature strain energy	relative CT activation (400 μM [lipid])
5.0	1.00	1.00
7.5	1.06	1.11
10.0	1.14	1.16
12.5	1.21	1.22
15.0	1.29	1.27

[a] Activity data is from two experiments performed in triplicate at 25 °C. The curvature strain calculations (eq 1) assumed a 7% increase in K_c between 5 and 15% DOG.

showed a very similar dependence on the amount of DOG present. Maximal CT activation by PC/DOG was approximately 3-fold lower than that seen with 60% DOPG/PC LUVs. Table 2 compares the calculated stored curvature strain energies of LUVs containing 5−15 mol % DOG with the CT activities measured in the presence of these LUVs at 25 °C. As seen with the PC/PE lipid systems, there is a good correlation between curvature strain energy and CT activity.

Lysophospholipids Reverse the Activation of CT by DAG. If CT were responding to the total stored curvature strain energy present in the membrane composed of class II lipids, it should be possible to reverse CT activation by the addition of a lipid with a spontaneous curvature of opposite sign. LysoPCs favor the formation of spherical micelles in water (*61*), which have positive curvature. Furthermore, addition of lysoPC has been shown to increase T_H of palmitoyl-oleoyl-PE (POPE), while DOG reduced T_H (*62*). The incorporation of a few mol % of lysoPC into monomethylDOPE LUVs at neutral pH is exothermic (*63*). The energy released is thought to be due to relief of stored curvature strain energy within the bilayer (*63*). The effects on the values of R_0 and K_c upon addition of oleoyl-lysoPC (OPC) or oleoyl-lysoPE (OPE) to DOPE monolayers have been determined (*64*). At 22 °C, R_0 changed from 29 to 34.8 Å (or 32.8 Å) as the mol % OPC (or OPE) increased from 0 to 10 mol %, while K_c was virtually unchanged. Thus both lysolipids decrease the negative curvature strain energy of this class II lipid system, with OPC being more potent than OPE.

Figure 5 shows that the addition of OPC or OPE to LUVs containing 10 mol % DOG in DOPC led to a progressive reversal of the DOG-induced activation. Thirteen mole percent OPC completely reversed activation by 10 mol % DOG. OPE was a less potent antagonist of DOG activation of CT than OPC, requiring a higher mole percent to produce equivalent inhibition of CT activation. This is in keeping with its weaker effect on negative curvature strain. The relative effects of these lysolipids on CT activation agree with a previous study, which demonstrated that the regulation of gramicidin channel function by lysolipids was due to their effects on membrane deformation energy (*65*). Lyso PC may reverse the effects of DAG on the binding of CT to cell membranes (*30*) and has been shown to inhibit CT activity in cells (*66*). The antagonism between class II activators and lipids that promote positive curvature further strengthens the proposal that curvature strain energy is a key regulatory parameter of CT.

Cholesterol is another class II lipid of potential importance in the regulation of CT's activity in vivo. In cultured fibroblasts, the rate of PC synthesis increased in cholesterol-enriched cells, as did the activity of membrane-bound CT (*67*). Free cholesterol loading of macrophages also induced CT activation and induction of PC biosynthesis (*68*); the authors suggested that this may be an important adaptive response for cell survival, attempting to prevent the free cholesterol:PC ratio from reaching a toxic level.

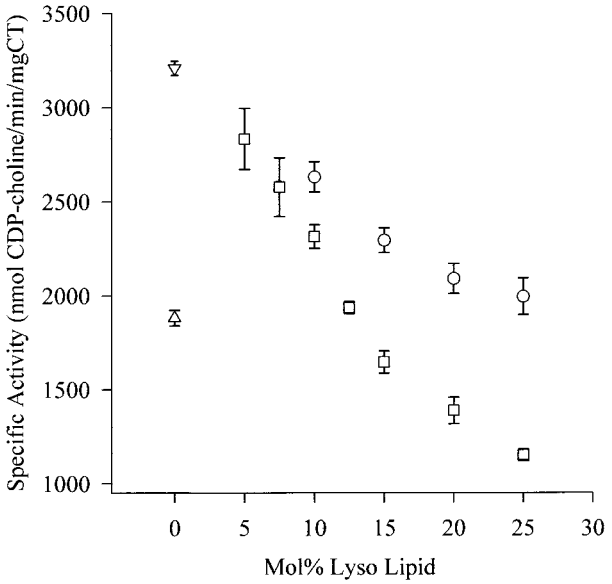

FIGURE 5: Oleoyl-lysophospholipids reverse the activation of CT by DOG. Assays were at 37 °C using 250 μM lipid. CT activity in the presence of pure DOPC LUVs (△), DOPC/10 mol % DOG (▽), DOPC/10 mol % DOG/5−25 mol % OPC (□), and DOPC/10 mol % DOG/10−25 mol % OPE (○). Error bars represent the standard error of the mean of six individual measurements.

The values of R_0 and K_c have been determined for a range of cholesterol-DOPC lipid mixtures (*52*). The relationship between monolayer spontaneous curvature and mole fraction cholesterol is linear (*52*). We can thus estimate the value of R_0 for monolayers containing various cholesterol contents. K_c for DOPC is 9 kT at 32 °C, and remains unchanged with the addition of cholesterol up to 30 mol %; addition of 50 mol % cholesterol to DOPC increases the value of K_c to 11 kT (*52*). Hence we can estimate the stored curvature strain energy of a range of DOPC/cholesterol LUVs. In the absence of tetradecane, DOPC with a cholesterol content of ≤50 mol % was shown to form only lamellar phases at 32 °C (*52*). On the basis of this information, we examined the effect on CT activity of 0−50 mol % cholesterol in DOPC LUVs at 32 °C, the temperature used for measuring the physical data. CT activity increased with cholesterol content to a maximum of 1.6-fold at 30 mol % cholesterol, and then fell again at 50 mol % cholesterol (data not shown). Table 3 summarizes the relative CT activation as a function of mole percent cholesterol and the relative stored curvature strain energies present in these different lipid membranes. Unlike our previous class II lipid systems, CT activation by DOPC/cholesterol LUVs did not correlate well with stored curvature strain energy; CT activation was much less than the increase in curvature strain energy. Clearly, some other membrane property is antagonizing the negative curvature effects on CT activity.

CT Activation Does Not Correlate with Access to the Hydrocarbon Core. Changes in surface polarity and surface voids leading to enhanced access to the acyl chains in membranes containing class II lipids were investigated using

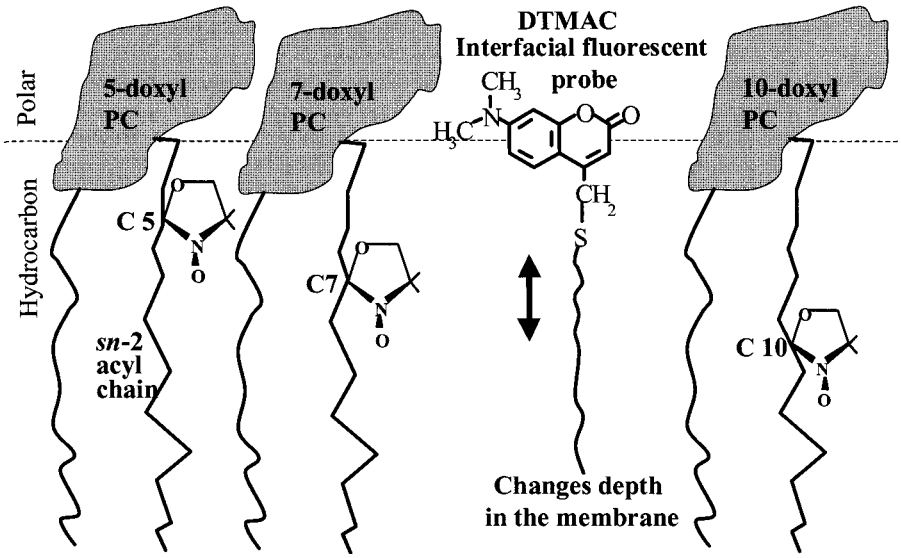

FIGURE 6: A schematic diagram of the quenching of DTMAC by a series of doxyl groups, attached at different positions to the *sn*-2 acyl chains of PC. This method gives information on the relative depth to which DTMAC penetrates into different lipid bilayers, which is a function of the polarity of the interfacial region, and provides a measure of the ease with which external molecules can access the membrane hydrocarbon core.

Table 3: Comparison of the Effects of 10−50 mol % Cholesterol in DOPC LUVs on the Relative Stored Curvature Strain Energy (Equation 1) and on the Relative CT Activation[a]

mol % cholesterol	relative curvature strain energy	relative CT activation	
		250 μM	500 μM
10	1.00	1.00	1.00
20	1.29	1.03	1.01
30	1.69	1.29	1.27
50	3.40	1.23	1.14

[a] The activity data is the mean of 6−13 individual measurements obtained at 32 °C.

a membrane tethered fluorophore, DTMAC (Figure 6). The DTMAC molecule can penetrate a membrane to a depth at which the membrane polarity matches the polarity of the coumarin ring (*69*). The emission wavelength of the DTMAC fluorophore is very sensitive to solvent polarity. Comparative analysis of DTMAC fluorescence in a variety of solvents and in PS/PC liposomes suggested that the coumarin fluorophore localizes within liposomes to a polarity equivalent to the glycerol backbone (*44*). That DTMAC adjusts its position to achieve polarity matching is supported by our finding that none of the lipid systems we tested significantly affected the wavelength of maximal emission (data not shown) but did influence the depth of penetration. The latter was assessed by measuring the degree of quenching of DTMAC fluorescence by a series of nitroxide-containing doxyl groups attached at different positions to the *sn*-2 acyl chains of PC and, thus, present at specific depths within the lipid bilayer (Figure 6). The depths of the doxyl quenchers are relatively fixed and the degree of quenching of DTMAC fluorescence by these labels is dependent upon the distance between probe and quencher. Thus, changes in DTMAC fluorescence quenching by doxyl-PCs as a function of lipid composition can reflect changes in the depth to which DTMAC penetrates bilayers of different composition. This provides a measure of alteration in two properties: the relative ease with which external molecules such as CT can access the membrane hydrocarbon core and the dielectric constant of the interfacial region of the bilayer (*69*).

The effects of increasing the DOPE content on the quenching of DTMAC by a series of doxyl-PCs is shown in Figure 7A. Quenching of the DTMAC fluorescence decreases as the mole percent PE is increased. This is seen with all three doxyl-PC systems, and is in good general agreement with a previous study of DTMAC quenching by 15 mol % 5-doxyl-PC in PC vs PE LUVs (*69*). If PE were creating surface packing voids that enhanced water permeation, DTMAC would have moved deeper into the bilayer to become more readily quenched by the doxyl probes buried in the membrane hydrocarbon region. Since we observed a reduction in DTMAC quenching, this suggests that DTMAC moves to a more superficial position upon introduction of the DOPE. This movement would be in keeping with an increased hydrophobicity of the PE/PC membrane interface, a feature confirmed by other findings showing that less water binds to PE bilayers than to pure PC bilayers (*70*). An alternative explanation for the reduction in quenching is that the doxyl probes become relatively immobilized as the proportion of class II lipid (DOPE) increases. However, this explanation is not supported by the lack of effect of another class II lipid, cholesterol (see below), which should be a stronger immobilizer than DOPE.

Figure 7B shows the quenching of DTMAC by doxyl-PCs in LUVs containing 60% of each of the three di-18:1 PEs. Quenching by all three nitroxyl groups showed the same trend, and was greatest in DOPE (Δ9) and least in DPLPE (Δ6). This agrees with a previous study, using 15 mol % 5-doxyl-PC and a PC/PE/PS lipid system (*71*). It also supports the findings of Berde and co-workers that the introduction of a double bond at position 9 to form cis-monounsaturated acyl chains produces maximal disruption of lipid chain packing (*72*). In agreement with a previous study (*71*), the presence of a double bond at the 6 position greatly reduces the accessibility of external substances to the bilayer interior. DVPE (Δ11) is the lipid that shows least CT binding and activation whereas DPLPE (Δ6) shows the

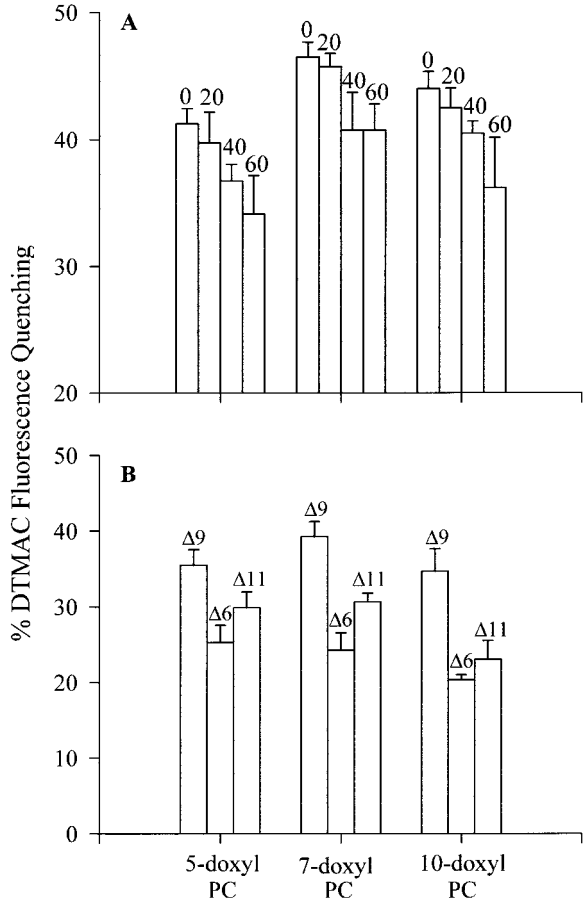

FIGURE 7: Quenching of DTMAC by a series of doxyl-PCs at 25 °C. (A) Effects of increasing the amount of DOPE in DOPC LUVs, The mol % DOPE is shown above the data. Error bars represent the standard error of the mean of 4−5 separate experiments. (B) Effects of a series of di-18:1 PEs (60% PE/40% DOPC). The position of the double bond is indicated above the data. Error bars represent the standard error of the mean of four individual experiments.

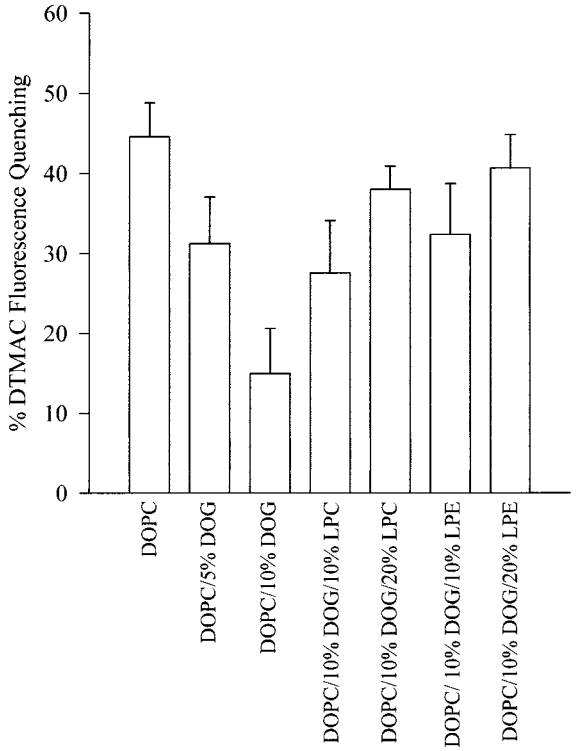

FIGURE 8: DTMAC quenching at 37 °C by 5% 7-doxyl-PC, present in LUVS containing the indicated lipids. Error bars represent the standard error of the mean of three independent experiments. Quenching data obtained using 5- or 10-doxyl-PC showed the same trend.

least DTMAC quenching. Access to the acyl chain regions of these PE lipid membranes does not correlate nearly as well with CT activation as their stored curvature strain energy values. The DTMAC results reported here and previously (*71*) suggest that the hydration order (i.e., order of DTMAC bilayer depth) for the di-18:1 PE series is Δ9 > Δ11 > Δ6; the CT activation order is Δ9 > Δ6 > Δ11. Thus, the hydration parameter also does not correlate with CT activity as well as does curvature strain.

Figure 8 shows the quenching of DTMAC fluorescence in DOPC/DOG and DOPC/DOG/lysolipid systems. DTMAC fluorescence quenching decreases as DOG increases from 0 to 10 mol %. However, addition of either lysolipid to DOPC/10 mol % DOG LUVs produces a progressive increase in DTMAC quenching. The polarity of the membrane interface has been suggested to increase with an increase in lysoPC content (*73*). As with the DOPC/DOPE systems, there appears to be a positive correlation between the activation of CT by these lipid systems and a decrease in the interfacial polarity of these bilayers.

We examined the quenching of DTMAC in DOPC LUVS containing 0−30 mol % cholesterol and found no significant differences in DTMAC quenching by all three doxyl-PCs (data not shown). There was a very significant decrease in DTMAC quenching with 50 mol % cholesterol; however, ethanol dilution tests (see Methods) revealed that the fluorescence of the DTMAC probe in this lipid system was subject to bleaching. After correction for this effect, the decrease in fluorescence quenching of DTMAC in DOPC/50 mol % cholesterol LUVs was minimal. Clearly, CT activation does not correlate well with access to cholesterol-containing bilayers. The effects of cholesterol on membrane hydration are complex. Cholesterol acts as a lateral spacer molecule, increasing the water uptake into the polar group region in a membrane (*74*). However, cholesterol has very little effect on membrane dipole potential or interbilayer hydration pressure (*74*), and 25 mol % cholesterol had little or no effect on surface interlipid hydrogen bonding (*75*). These findings suggest that, although there is more water present in the voids created by cholesterol at the surface of a PC/cholesterol membrane, the amount of bound water may change very little. Furthermore, the polarity of a cholesterol molecule's "headgroup" region is less than that of a PC headgroup. Thus, membrane interfacial hydrophobicity may change very little with cholesterol content. In addition, the access to the bilayer interface may change very little, or even decrease because of a "stiff" membrane. The lack of any significant differences in DTMAC quenching with DOPC/cholesterol LUVs agrees with these findings.

CONCLUSIONS

Class II lipids induce negative curvature strain, surface voids, increased lateral pressure in the acyl chain region, and dehydration of the headgroup region. In all systems we tested, except for cholesterol, the best correlation with CT activation was negative curvature strain. The stored curvature strain energy may affect the free energy of binding by facilitating

the expansion of the lipid bilayer required for peptide insertion (*76*). It may also provide a source of energy for a conformational change in the enzyme (*9*).

Access of a fluorescent probe to the bilayer interior did not correlate well with CT's activation by the class II lipid membranes used in this study. Although looser packing may, along with negative charge, participate in the activation of CT by anionic lipids, its role in the activation by class II lipids is less certain. In fact, class II lipids increase packing pressure in the acyl chain region, and in the case of PE, promote headgroup H-bonding interactions. CT's lack of response to packing properties contrasts to protein kinase C, for which lipid packing properties are of greater importance than membrane stored curvature strain energy (*71*, *77*).

The reduction in DTMAC quenching by class II lipids correlated well with CT activation when the changes in lipid physical properties were large, such as the addition of DOG. However, when the lipid structural changes were small, e.g., variation in the double bond positioning of the di-18:1 PE isomers, curvature strain correlated more closely with activation. The changes in DTMAC positioning may probe the changes in the hydrophobicity (degree of hydration) at the membrane interface. PE membranes show decreased surface and interchain hydration (*39*). PE headgroups tend to hydrogen bond with each other, at the expense of lipid-water hydrogen bond formation. Thus, the interface of PE membranes will be less polar. Similarly, DAGs decrease the hydration of the bilayer surface and increase exposure of membrane hydrophobic chains (*76*, *78*), which will increase membrane interfacial hydrophobicity. Hydrophobic interactions dominate the energetics of CT's interactions with lipid membranes (*27*, *79*). The binding of domain M to a surface displaying less bound water would facilitate the hydrophobic interaction of the nonpolar face of the domain M amphipathic helix.

CT activation by cholesterol-containing membranes was less than expected from calculation of their relative stored curvature strain energies, suggesting antagonism by some other cholesterol-induced membrane property. Cholesterol did not significantly change surface hydrophobicity as assessed by DTMAC fluorescence quenching. In addition, cholesterol increases acyl chain order in lipid membranes, and based on a previous study (*40*), this ordering should antagonize CT binding. Thus, in addition to negative curvature strain, both the lack of effects on surface hydrophobicity and the increase in chain ordering could contribute to the net effects of cholesterol on CT's activity.

In conclusion, our study provides strong experimental evidence for a primary role of membrane curvature strain and a secondary role for surface dehydration in signaling CT's binding to class II lipid membranes. In that CT activation stimulates synthesis of bilayer forming PC, its sensitivity to these physical properties of nonbilayer lipids provides a mechanism for homeostatic control of membrane curvature strain.

ACKNOWLEDGMENT

Grateful thanks to Dr. Joanne Johnson for CT purification, to Dr. Peter Rand for providing us with pre-publication structural data on the lysolipids used in this paper, and also to Dr. Erwin London for helpful discussions regarding the application of nitroxide-labeled phospholipid quenchers.

REFERENCES

1. Jackowski, S. (1996) *J. Biol. Chem. 271*, 20219−20222.
2. Morein, S., Andersson, A.-S., Rilfors, L., and Lindblom, G. (1996) *J. Biol. Chem. 271*, 6801−6809.
3. Österberg, F., Rilfors, L., Wieslander, A., Lindblom, G., and Gruner, S. M. (1995) *Biochim. Biophys. Acta 1257*, 18−24.
4. Thurmond, R. L., Niemi, A. R., Lindblom, G. Wieslander, A., and Rilfors, L. (1994) *Biochemistry 33*, 13178−13188.
5. Vikström, S., Li, L., and Wieslander, Å. (2000) *J. Biol. Chem. 275*, 9296−9302.
6. Vikström, S., Li, L., Karlsson, O. P., and Wieslander, Å. (1999) *Biochemistry 38*, 5511−5520.
7. McCallum, C. D., and Epand, R. M. (1995) *Biochemistry 34*, 1815−1824.
8. Li, L., Zheng, L. X., and Yang, F. Y. (1995) *Chem. Phys. Lipids 76*, 135−144.
9. Brown, M. F. (1994) *Chem. Phys. Lipids 73*, 159−180.
10. Burack, W. R., and Biltonen, R. L. (1994) *Chem. Phys. Lipids 73*, 209−222.
11. Schwarz, D., Disselev, P., Wessel, R., Jueptner, O., and Schmid, R. D. (1996) *J. Biol. Chem. 271*, 12840−12846.
12. Mosier, M., and Epand, R. M. (1999) *J. Liposome Res. 9*, 21−42.
13. Kent, C. (1997) *Biochim. Biophys. Acta 1348*, 79−90.
14. Friesen, J. A., Campbell, H. A., and Kent, C. (1999) *J. Biol. Chem. 274*, 13384−13389.
15. Yang, W., Boggs, K. P., and Jackowski, S. (1995) *J. Biol. Chem. 270*, 23951−23957.
16. Cornell, R. B., and Northwood, I. C. (2000) *Trends Biochem. Sci. 25*, 441−447.
17. Cornell, R. B. (1998) *Biochem. Soc. Trans. 26*, 539−544.
18. Cornell, R. B., and Arnold, R. S. (1996) *Chem. Phys. Lipids 81*, 215−227.
19. Dunne, S., Cornell, R. B., Johnson, J. E., Glover, N. R., and Tracey, A. S. (1996) *Biochemistry 35*, 11975−11984.
20. Johnson, J. E., Aebersold, R., and Cornell, R. B. (1997) *Biochim. Biophys. Acta 1324*, 273−284.
21. Feldman, D. A., Brubaker, P. G., and Weinhold, P. A. (1981) *Biochim. Biophys. Acta 665*, 53−59.
22. Sleight, R. G., and Kent, C. (1983) *J. Biol. Chem. 258*, 836−839.
23. Cornell, R. B., and Vance, D. E. (1987) *Biochim. Biophys. Acta 919*, 26−36.
24. Utal, A. K., Jamil, H., and Vance, D. E. (1991) *J. Biol. Chem. 266*, 24084−24091.
25. Cornell, R. B. (1991) *Biochemistry 30*, 5873−5880.
26. Cornell, R. B. (1991) *Biochemistry 30*, 5881−5888.
27. Arnold, R. S., and Cornell, R. B. (1996) *Biochemistry 35*, 9917−9924.
28. Arnold, R. S., Depaoli-Roach, A., and Cornell, R. B. (1997) *Biochemistry 36*, 6149−6156.
29. Sleight, R. G., and Dao, H.-N. T. (1990) *Lipids 25*, 100−107.
30. Jamil, H., Hatch, G., and Vance, D. E. (1993) *Biochem. J. 291*, 419−427.
31. Attard, G. S., Templer, R. H., Smith, W. S., Hunt, A. N., and Jackowski, S. (2000) *Proc. Natl. Acad. Sci. 97*, 9032−9036.
32. Israelachvili, J. N., Marcelja, S., and Horn, R. G. (1980) *Q. Rev. Biophys. 13*, 121−200.
33. Cantor, R. S. (1999) *Chem. Phys. Lipids 101*, 45−56.
34. Helfrich, W. (1973) *Z. Naturforsch. 28C*, 693−703.
35. Gruner, S. M., Parsegian, V. A., and Rand, R. P. (1986) *Faraday Discuss. Chem. Soc. 81*, 29−37.
36. Rand, R. P., Fuller, N. L., Gruner, S. M., and Parsegian, V. A. (1990) *Biochemistry 29*, 76−87.
37. Nielsen, C., and Andersen, O. S. (2000) *Biophys. J. 79*, 2583−2604.
38. Johnson, J. E., and Cornell, R. B. (1994) *Biochemistry 33*, 4327−4335.
39. Ho, C., Slater, S. J., and Stubbs, C. D. (1995) *Biochemistry 34*, 6188−6195.

40. Drobnies, A. E., van der Ende, B., Thewalt, J. L., and Cornell, R. B. (1999) *Biochemistry 38*, 15606−15614.
41. Hope, M. J., Bally, M. B., Webb, G., and Cullis, P. R. (1985) *Biochim. Biophys. Acta 812*, 55−65.
42. Bartlett, G. R. (1959) *J. Biol. Chem. 234*, 466−468.
43. Cornell, R. B. (1989) *J. Biol. Chem. 264*, 9077−9082.
44. Sterk, G. J., Thijsse, P. A., Epand, R. F., Wong Fang Sang, H. W., Kraayenhof, R., and Epand, R. M. (1997) *J. Fluoresc. 7*, 115S−118S.
45. MacDonald, J. I., and Kent, C. (1993) *Protein Expression Purif. 4*, 1−7.
46. Sohal, P. S., and Cornell, R. B. (1990) *J. Biol. Chem. 265*, 11746−11750.
47. Laemmli, U.K. (1970) *Nature 227*, 680−685.
48. Kachel, K., Asuncion-Punzalan, E., and London, E. (1998) *Biochim. Biophys. Acta 1374*, 63−76.
49. Sleight, R. G., and Kent, C. (1983) *J. Biol. Chem. 258*, 831−835.
50. Weinhold, P. A., Rousifer, M. E., and Feldman, D. A. (1986) *J. Biol. Chem. 261*, 5104−5110.
51. Tilcock, C. P. S., Bally, M. B., Farren, S. B., and Cullis, P. R. (1982) *Biochemistry 21*, 4596−4601.
52. Chen, Z., and Rand, R. P. (1997) *Biophys. J. 73*, 267−276.
53. Kozlov, M. M., Leikin, S., and Rand, R. P. (1994) *Biophys. J. 67*, 1603−1611.
54. Marsh, D. (1996) *Biophys. J. 70*, 2248−2255.
55. Kozlov, M. M., and Helfrich, W. (1992) *Langmuir 8*, 2792−2797.
56. Keller, S. L., Bezrukov, S. M., Gruner, S. M., Tate, M. W., Vodyanoy, I., and Parsegian, V. A. (1993) *Biophys. J. 65*, 23−27.
57. Epand, R. M., Fuller, N., and Rand, R. P. (1996) *Biophys. J. 71*, 1806−1810.
58. Slack, B. E., Breu, J., and Wurtman, R. J. (1991) *J. Biol. Chem. 266*, 24503−24508.
59. Tronchère, H., Planat, V., Record, M., Tercé, F., Ribbes, G., and Chap, H. (1995) *J. Biol. Chem. 270*, 13138−13146.
60. Leikin, S., Kozlov, M. M., Fuller, N. L., and Rand, R. P. (1996) *Biophys. J. 71*, 2623−2632.
61. Rand, R. P., Pangborn, W. A., Purdon, A. D., and Tinker, D. O. (1975) *Can. J. Biochem. 53*, 189−195.
62. Epand, R. M. (1985) *Biochemistry 24*, 7092−7095.
63. Epand, R. M., and Epand, R. F. (1994) *Biophys. J. 66*, 1450−1456.
64. Fuller, N., and Rand, R. P. (2001) *Biophys. J. 81*, 243−254.
65. Lundbaek, J. A., and Andersen, O. S. (1994) *J. Gen. Physiol. 104*, 645−673.
66. Boggs, K. P., Rock, C. O., and Jackowski, S. (1995) *J. Biol. Chem. 270*, 7757−7764.
67. Leppimäki, P., Mattinen, J., and Slotte, J. P. (2000) *Eur. J. Biochem. 267*, 6385−6394.
68. Zhang, D., Tang, W., Yao, P. M., Yang, C., Xie, B., Jackowski, S., and Tabas, I. (2000) *J. Biol. Chem. 275*, 35368−35376.
69. Epand, R. F., Kraayenhof, R., Sterk, G. J., Wong Fong Sang, H. W., and Epand, R. M. (1996) *Biochim. Biophys. Acta 1284*, 191−195.
70. McIntosh, T. J., and Simon, S. A. (1994) *Annu. Rev. Biophys. Biomol. Struct. 23*, 27−51.
71. Giorgione, J. R., Kraayenhof, R., and Epand, R. M. (1998) *Biochemistry 37*, 10956−10960.
72. Berde, C. B., Andersen, H. C., and Hudson, B. S. (1980) *Biochemistry 19*, 4279−4293.
73. Sheffield, M. J., Baker, B. L., Li, D., Owen, N. L., Baker, M. L., and Bell, J. D. (1995) *Biochemistry 34*, 7796−7806.
74. McIntosh, T. J., Magid, A. D., and Simon, S. A. (1989) *Biochemistry 28*, 17−25.
75. Slater, S. J., Ho, C., Taddeo, F. J., Kelly, M. B., and Stubbs, C. D. (1993) *Biochemistry 32*, 3714−3721.
76. Kinnunen, P. K. J. (1991) *Chem. Phys. Lipids 57*, 375−399.
77. Giorgione, J. R., Huang, Z., and Epand, R. M. (1998) *Biochemistry 37*, 2384−2392.
78. Goñi, F. M., and Alonso, A. (1999) *Prog. Lip. Res. 38*, 1−48.
79. Johnson, J. E., Rao, N. M., Hui, S. W., and Cornell, R. B. (1998) *Biochemistry 37*, 9509−9519.

BI010904C